

# Observation of non-gyrotropy of electrons caused by wave-particle interaction with intense whistler mode waves in mirror mode structures in the magnetosheath

N. Kitamura<sup>1</sup>, M. Kitahara<sup>2</sup>, S. A. Boardsen<sup>3,4</sup>, T. Amano<sup>1</sup>, D. J. Gershman<sup>3</sup>, Y. Omura<sup>5</sup>, S. Nakamura<sup>2</sup>, M. Shoji<sup>2</sup>, Y. Katoh<sup>6</sup>, H. Kojima<sup>5</sup>, Y. Miyoshi<sup>2</sup>, Y. Saito<sup>7</sup>, M. Hirahara<sup>2</sup>, S. Yokota<sup>8</sup>, B. L. Giles<sup>3</sup>, W. R. Paterson<sup>3</sup>, C. J. Pollock<sup>9</sup>, O. Le Contel<sup>10</sup>, C. T. Russell<sup>11</sup>, N. Ahmadi<sup>12</sup>, P.-A. Lindqvist<sup>13</sup>, R. E. Ergun<sup>12</sup>, and J. L. Burch<sup>14</sup>

1. Department of Earth and Planetary Science, Graduate School of Science, the University of Tokyo, Tokyo, Japan. 2. Institute for Space-Earth Environmental Research, Nagoya University, Nagoya, Japan. 3. NASA Goddard Space Flight Center, Greenbelt, Maryland, USA. 4. Goddard Planetary Heliophysics Institute, University of Maryland, Maryland, USA. 5. Research Institute for Sustainable Humanosphere, Kyoto University, Uji, Japan. 6. Department of Geophysics, Graduate School of Science, Tohoku University, Sendai, Japan. 7. Institute of Space and Astronautical Science, Japan Aerospace Exploration Agency, Sagamihara, Japan. 8. Department of Earth and Space Science, Graduate School of Science, Osaka University, Toyonaka, Japan. 9. Denali Scientific, Fairbanks, Alaska, USA. 10. Laboratoire de Physique des Plasmas, CNRS/Ecole Polytechnique/Sorbonne Université/Université Paris-Sud/Observatoire de Paris, Paris, France. 11. Department of Earth, Planetary, and Space Science, University of California, Los Angeles, California, USA. 12. Laboratory for Atmospheric and Space Physics, University of Colorado, Boulder, Colorado, USA. 13. Royal Institute of Technology, Stockholm, Sweden. 14. Southwest Research Institute, San Antonio, TX, USA.

## 1. Introduction

### Whistler mode waves in magnetic field intensity troughs in the magnetosheath

- Frequency below electron cyclotron frequency ( $\sim 0.1\text{--}0.5 f_{ce}$ )
- R-mode polarization and small wave normal angle in most cases
- Generated from electron temperature anisotropy ( $T_{e,para} < T_{e,perp}$ )
- Generated around minimum-B along a field-line

[e.g., Zhang et al., 1998; Baumjohann et al., 1999; Giagkiozis et al., 2018]

**Resonance condition (cyclotron resonance)**

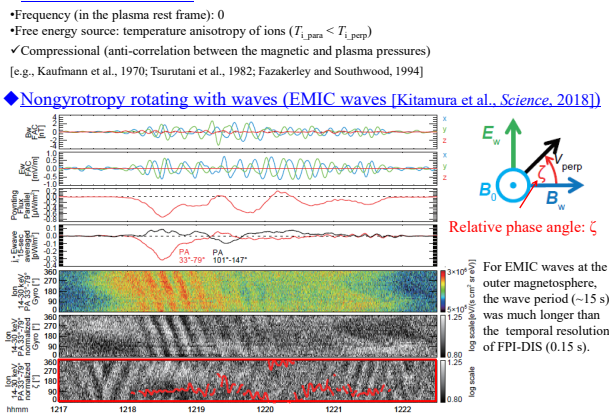
$V_R$ : Resonance velocity  
 $\omega$ : Wave angular frequency  
 $\Omega_{ce}$ : Electron cyclotron angular frequency  
 $V_R = \omega - \Omega_{ce}/k_{para}$

**Mirror mode structures**

• Frequency (in the plasma rest frame): 0  
 • Free energy source: temperature anisotropy of ions ( $T_{i,para} < T_{i,perp}$ )  
 • Compressional (anti-correlation between the magnetic and plasma pressures)

[e.g., Kaufmann et al., 1970; Tsurutani et al., 1982; Fazakerley and Southwood, 1994]

**Nongyrotropy rotating with waves (EMIC waves [Kitamura et al., Science, 2018])**



To identify nongyrotropy rotating with the wave is the first step to investigate energy exchange between the wave and particles in detail.

Here, we show observations of nongyrotropy of electrons during an intense whistler mode wave event in the magnetosheath.

## 2. Dataset and Analysis Method

- **FGM**: 16 vectors/s (Fast Survey) (Used as the background magnetic field ( $B_0$ ))
  - **SCM**: 8192 vectors/s (Burst data)
  - **EDP**: 8192 vectors/s (Burst data)
  - **FPI-DES**: Time-tagged data (v3.4.0) (Not lossy compressed interval only) ( $\sim 195 \mu\text{s}/\text{step} \ll \text{wave period} \sim 10 \text{ ms} < 30 \text{ ms}$  (Original temporal resolution of DES))
- Angular resolution:  $11.25^\circ$  (32 (Azimuth)  $\times$  16 (Elevation) (=512) pixels)  
 Spacecraft separation:  $\sim 7 \text{ km}$  ( $<$  wavelength of whistler mode waves)  
 Data from all spacecraft are combined after a correction using relative total electron pressures.
1. Some correction of look directions and additional flat fielding in gyro direction
  2. Sort by relative phase angle ( $\zeta$ ) and average differential energy fluxes ( $F$ ) in each  $22.5^\circ$  bin
  3. Normalization by averaged differential energy flux ( $F_{avg}$ ) (average of 3 original data ( $\sim 90 \text{ ms}$ ) at all  $\zeta$  bins in each energy and pitch angle ( $11.25^\circ$  resolution) bin)
- Significance of  $F - F_{avg}$  in each  $\zeta$  bin are estimated as  $(F - F_{avg}) \sqrt{N} / F_{avg}$ , where  $N$  is the total of counts.

## 4. Result

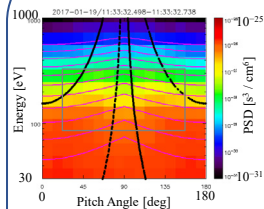


Fig. Phase space densities (PSD) with cyclotron and Landau resonance velocities, and some diffusion curves

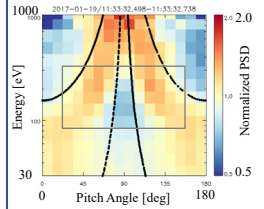
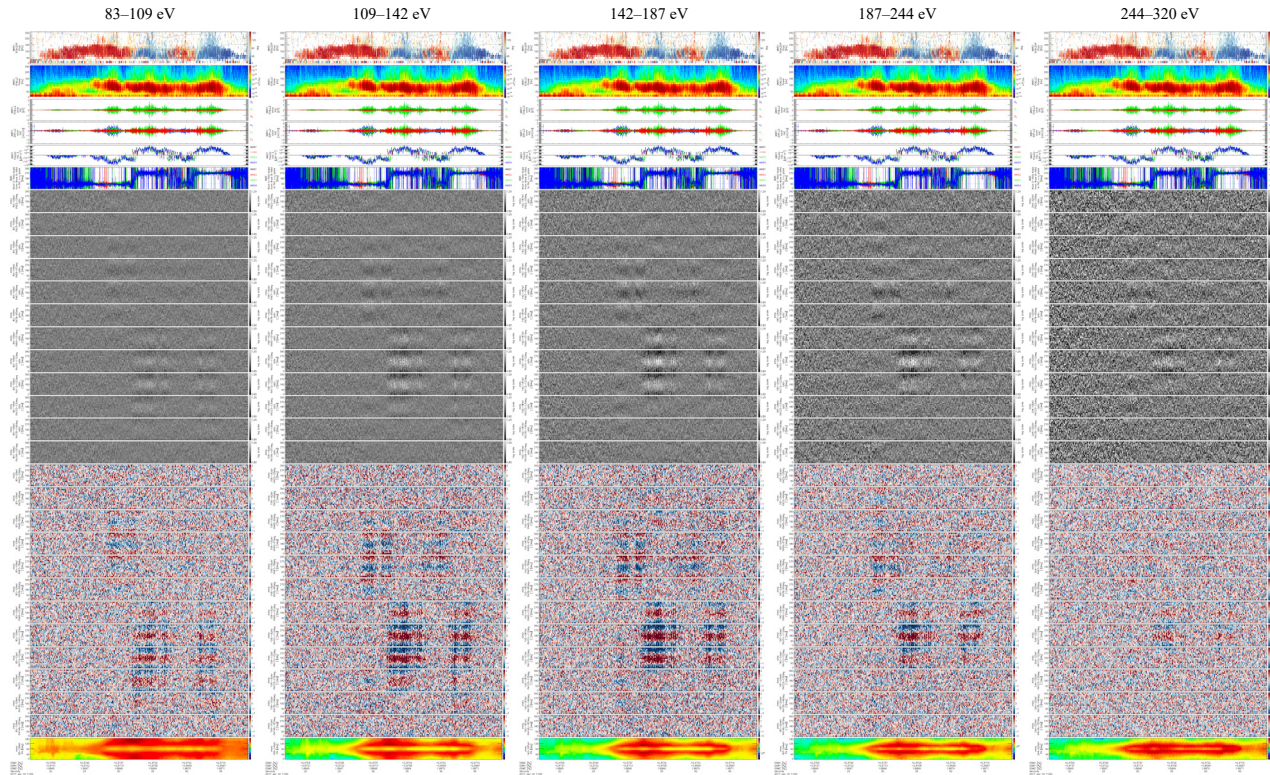


Fig. PSD normalized by the average of those in each energy bin with cyclotron and Landau resonance velocities

At low energies ( $< 100 \text{ eV}$ ), the PSD is large in the direction parallel to the magnetic field. At medium energies (several hundred electron volts) it shows a butterfly distribution. At relatively high energies ( $\sim 1 \text{ keV}$ ) it shows a pancake distribution. [e.g., Kitamura et al., JGR, 2020]

Around the cyclotron resonance velocity, the PSD tends to be larger on the side near the pitch angle of  $90^\circ$ .  
 → Preferable for the growth of whistler mode waves

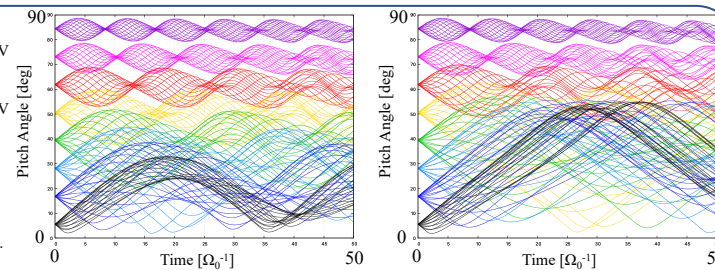


Figs. Spectrum (0–250 Hz) of angle between the pointing flux and the magnetic field, power spectrum (0–250 Hz) of the magnetic field (MMS1 SCM), the magnetic field waveform (MMS1 SCM), the electric field waveform (MMS1 EDP), the parallel component of the pointing flux to the magnetic field, phase of the wave electric field with respect to the wave magnetic field,  $\zeta$ -dependence of the normalized electron distribution in each  $11.25^\circ$  pitch angle ( $22.5^\circ\text{--}167.5^\circ$ ) (color range: 0.8–1.25), significance of deviation from gyro-averaged flux in each  $11.25^\circ$  pitch angle bins ( $22.5^\circ\text{--}167.5^\circ$ ) (color range:  $-2\text{--}2$ ), and pitch angle distribution of electrons.

## 4. Discussion

A characteristic non-gyrotropic  $\zeta$ -distribution of electrons is identified at the velocity much slower than the cyclotron resonance (apparently outside the trapping velocity around the resonance), and the region corresponds roughly to the side where the pitch angle is closer to  $90^\circ$  than the peak of the butterfly distribution.  
 → Distortion of the pitch angle distribution associated with non-resonant interaction probably appears as the characteristic  $\zeta$ -distribution.

Left:  
 Energy = 96.34 eV  
 $(v_e = 5821 \text{ km/s})$   
 Right:  
 Energy = 165.1 eV  
 $(v_e = 7621 \text{ km/s})$   
 $f_{\perp}^2/f_{\parallel}^2 = 79$   
 $B_w/B_0 = 0.03$   
 Various initial  $\zeta$   
 (Calculated by M. Kitahara)



## 5. Conclusion

- Non-gyrotropy of electrons associated with the non-resonant interaction was observed.
- The non-gyrotropy was much clearer than that around the cyclotron resonance or Landau resonance, even if it exists.